Piezoelectric Performance of Piezoceramic-Polymer Composites with 2-2 Connectivity— A Combined Theoretical and Experimental Study

Q. M. Zhang, Wenwu Cao, J. Zhao, and L. E. Cross, *Fellow, IEEE*

Abstract—**The piezoelectric performance of piezoceramic polymer composites with 2-2 connectivity at low frequency has been analyzed theoretically. Due to the elastic coupling between the ceramic and polymer phases, the strain components in directions perpendicular and parallel to the ceramic-polymer interface are not uniform in either phases. As a result, most of the stress transfer between the two phases occurs at the region near the surface of the composite. In order to improve the piezoelectric performance of a composite, the polymer matrix should have a small Young's modulus and a large shear modulus, and a large aspect ratio. It may be also desirable to have the polymer matrix made of two different polymers with the stiffer one near the surface and the softer one in the interior of the composite. To compare with the theoretical calculations, surface profiles of a series of 2-2 composites with different aspect ratios were measured, and the experimental results show excellent agreement with the theoretical calculations. The nonuniform strain and stress in the direction parallel to the ceramic-polymer interface of a composite were also confirmed by experiments.**

I. Introduction

ONE OF THE KEY design criteria of piezoceramic polymer composites is to optimize the stress transfer between the two constituents—the piezoelectric ceramic and polymer matrix. Since the stress transfer between the two constituents depends on the dimensions and elastic properties of each phase in a complicated manner, as has been demonstrated by numerous experiments, there has been a constant effort to establish a quantitative understanding of how various design parameters affect the performance of a piezocomposite [1]–[5]. One of the most frequently used models in analyzing the properties of a composite is based on the isostrain approximation, i.e., the assumption that the elastic displacements in the two constituents are equal in the ceramic poling direction. However, the results derived using the isostrain approximation often overestimated the stress transfer between the two phases. Also, the prediction that the piezoelectric performance of a composite should be independent of the aspect ratio of the ceramics in a composite, derived from the isostrain approximation, was apparently incorrect. As a matter of fact, the aspect ratio is one of the most important parameters in adjusting the performance of a composite [3],[5].

Manuscript received July 20, 1993; revised February 24, 1994. This work was supported by the Office of Naval Research through Grant N00014-93-1-0340.

The authors are with the Materials Research Laboratory, The Pennsylvania State University, University Park, PA 16802 USA.

IEEE Log Number 9401997.

Recently, in an effort to improve the modeling of piezocomposites, we have introduced a simple model based on the static force balance condition to describe the mechanical and the piezoelectric response of a composite under external stress or electric fields [6], [7].The model provided the trend of how the elastic properties of each phase and especially the aspect ratio of the ceramics affect the performance of a composite, and was in good agreement with experimental results. Hence, it provided a much better base for relating the performance of a composite to the design parameters. However, quantitatively, there still existed some discrepancy between experimental results and theoretical predictions. For example, in order to fit the experimental surface profile of a composite, a much larger Poisson's ratio for the polymer matrix has to be used. The discrepancies are the result of the approximation made in the model that the strain in both phases along the piezoceramic poling direction (the z-direction, as will be introduced later in this paper) is a constant (or independent of z-coordinate). In this paper, we will eliminate this assumption and treat the piezocomposites using the basic static elastic equations: [8]

$$\sum_{k=1}^{3} \frac{\partial T_i k}{\partial x_k} = 0 \tag{1}$$

In (1), i and $k = 1, 2$, and 3 (or x, y, and z as will be used later in this paper) correspond to the three orthogonal coordinates x, y, and z. Although a standard procedure for solving (1) has been developed, it involves complicated mathematical calculations for a composite structure, which quite often do not yield much physical insight [9]. To avoid this, numerous approximations were made in the literature to simplify (1) so that a closed form solution can be obtained for composites [10]–[12]. In trying to adapt these results to the piezoceramic polymer composites, we found that among these theoretical studies, there is a common shortcoming, i.e., there always exists an undetermined adjustable parameter in the final results, which is not desirable for a model required to give quantitative predictions.

For a piezocomposite with 2-2 connectivity, as shown in Fig. 1, we will show in this paper that one can greatly simplify (1) by making use of the features of a typical 2-2 composite. The calculated results from this approach indicate that the strain field in both the x and z-directions is not uniform. It also shows that most of the stress transfer between the two constituents occurs near the surface of a composite. The results

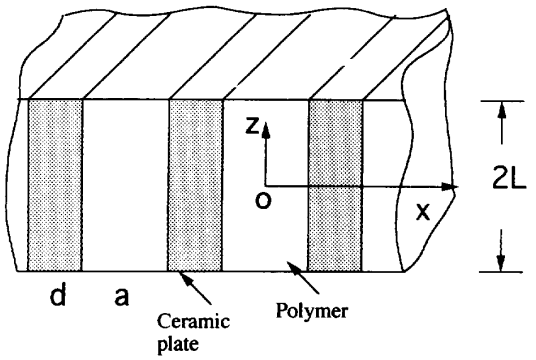

Fig. 1. Schematic drawing of a 2-2 piezoceramic-polymer composite. The ceramic plates are marked by shaded areas, the width of ceramic plate is d and the width of polymer matrix gap is a and the sample thickness is $2L$. z is the poling direction of the ceramic plate.

confirm that when a composite thickness $2L$ is much larger than the width of ceramic plates and polymer gap (d and a), the performance of a composite at low frequency can be analyzed by the isostrain approximation.

In order to compare with the theoretical results, we have also carried out a series of measurements on the surface profile of 2-2 composites with different aspect ratio using a double beam laser dilatometer [13]. The theoretically calculated profile and experimentally measured one agree with each other in numerical value even without use of adjustable parameters. We have also made a 2-2 composite with multilayer structure so that the z-dependence of the local stress field can be probed and the result also agrees with the theoretical prediction. It is conceivable that the method used here to measure the local stress field may be generalized to the structure composites in which the piezoceramic elements can serve as sensors to monitor the change in the local stress field. In this manner, one may be able to verify the detailed theoretical predictions about the stress pattern in these composites.

II. Piezoelectric Response of 2-2 Composites Under an Electric Field

In the earlier publication, [6] we have shown that when a composite is subjected to an external electric field along the ceramic poling direction, the surface displacement profile is not uniform. The displacement in the polymer region is always less than that in the piezoceramic region. From this nonuniform strain distribution, one is able to calculate the stress transfer between the two phases [6], [7]. Since the ceramic plates are poled in the z-direction, we are mainly concerned with the stress transfer in that direction. Hence, we only consider the following elastic equation

$$\frac{\partial T_{zz}}{\partial z} + \frac{\partial T_{xz}}{\partial x} = 0 \tag{2}$$

As shown in Fig. 1 the y-dimension of a typical 2-2 composite is much larger than the thickness $2L$ and repeating distance $(a + b)$ in the x-direction of the composite, hence all the quantities involved are assumed to be independent of y-coordinate. Through the stress-strain relationship, (2) can be converted to [10]

$$(\lambda + \mu)\frac{\partial \varepsilon}{\partial z} + \mu \nabla^2 u_z = 0 \tag{3}$$

where λ and μ are the Lame coefficients (μ is the shear modulus), $\varepsilon = u_{xx} + u_{yy} + u_{zz}$, and ∇^2 is the Laplacian operator. For simplicity, we assume that both ceramic and polymer are elastically isotropic (the elastically anisotropic case can also be treated utilizing the procedure outlined in this paper). λ and μ are related to the Young's modulus Y and Poison's ratio σ through

$$\mu = \frac{Y}{2(1+\sigma)}$$

and

$$\lambda = \frac{Y\sigma}{(1+\sigma)(1-2\sigma)}$$

When an electric field E_3 (E_3 is a constant) is applied on a composite, one has the following constitutive relations in the ceramic:

$$T_{xx} = c_{11}^c u_{xx} + c_{12}^c u_{yy} + c_{12}^c u_{zz} - e_{31}E_3 \tag{4a}$$

$$T_{yy} = c_{12}^c u_{xx} + c_{11}^c u_{yy} + c_{12}^c u_{zz} - e_{31}E_3 \tag{4b}$$

$$T_{zz} = c_{12}^c u_{xx} + c_{12}^c u_{yy} + c_{11}^c u_{zz} - e_{33}E_3 \tag{4c}$$

where c_{ij}^c are the elastic constants (the superscript c refers to the ceramic) and e_{ij} are the piezoelectric stress constants for the ceramic. Similar equations can be written for the polymer matrix except that all $e_{ij} = 0$ and c_{ij} are those for the polymer.

From earlier experimental and theoretical results and the dimensionality arguments, the strain u_{yy} in both polymer matrix and ceramic plate can be assumed to be constant. For a composite material, in general, T_{xx} is not equal to zero when it is subjected to an electric field. However, this non-zero T_{xx} is the result of the stress transfer in the z-direction between the two constitunents and it is, therefore, small compared with the stress in the z-direction. Since we are mostly concerned with the stress transfer in the z-direction, the error of assuming $T_{xx} = 0$ to the z-direction stress transfer will be on the order of σ^2(σ is the Poisson's ratio). [6] Under these approximations, the strain u_{xx} and u_{zz} are related by

$$u_{xx} = \frac{-1}{c_{11}^c}(c_{12}^c A_y + c_{12}^c u_{zz} - e_{31}E_3) \tag{5a}$$

$$u_{xx} = \frac{-1}{c_{11}^p}(c_{12}^p A_y + c_{12}^p u_{zz}) \tag{5b}$$

where (5a) is for the ceramic plate and (5b) for the polymer matrix. u_{yy} is the same in both phases and is denoted as a constant A_y. Substituting (5) to (3) yields

$$K^2 \frac{\partial^2 u_z}{\partial z^2} + \frac{\partial^2 u_z}{\partial x^2} = 0 \tag{6}$$

where

$$K_2 = [(\lambda + 2\mu) - (\lambda + \mu)\lambda/c_{11}]/\mu = Y(2 - \sigma)/[2\mu(1 - \sigma^2)] \quad (7)$$

(6) can be used for both ceramic plate and polymer matrix, except different elastic constants should be used for different phases. Apparently, u_z is a function of both x and z. Following the standard procedure in solving the partial differential equation, we assume u_z as $u_z = f(x)g(z)$. Substituting this into (6), one gets two ordinary differential equations:

$$\frac{K^2}{g(z)}\frac{\partial^2}{\partial x^2}g(z) = -\beta^2$$

and

$$\frac{1}{f(x)}\frac{\partial^2}{\partial x^2}f(x) = \beta^2 \quad (8)$$

The solution to (8) which satisfies the boundary condition that $u_z = 0$ at $z = 0$, and the symmetry of the problem $\frac{\partial u_z}{\partial x} = 0$ at $x = 0$ for the polymer matrix and at $x = (a + d)/2$ for the ceramic plate is

$$u_z^c = A^c z + \sum_{n=0}^{\infty} B_n^c \sin(\alpha_n z)\cosh[\beta_n^c(x - (a + d)/2] \quad \left(\frac{a}{2} \le x \le d + \frac{a}{2}\right) \quad (9a)$$

$$u_z^p = A^p z + \sum_{n=0}^{\infty} B_n^p \sin(\alpha_n z)\cosh(\beta_n^p x) \quad \left(\frac{-a}{2} \le x \le \frac{a}{2}\right) \quad (9b)$$

where A^c, A^p, B_n^c, and B_n^p are the integration constants, $\beta_n^c = K^c\alpha_n$ and $\beta_n^p = K^p\alpha_n$. α_n is the eigenvalue, which will be determined from the boundary condition. K^c and K^p are defined in (7) for the ceramic plate and polymer matrix, respectively. Due to the periodic nature of the composite, we only write down the solution for a unit cell of the composite at $-a/2 < x < a/2 + d$.

The following boundary conditions are used to determine the integration constants:

$$T_{zz} = 0 \text{ at } z = \pm L,$$
$$u_{zz}^c = u_{zz}^p \text{ and } T_{xz}^c = T_{xz}^p \text{ at } x = a/2,.$$
$$u_{yy}^c = u_{yy}^p = A_y.$$

The relation between the shear stress T_{xz} and the shear strain u_{xz} is

$$T_{xz} = \mu\left(\frac{\partial u_z}{\partial x} + \frac{\partial u_x}{\partial z}\right)$$

Making use of (4) and (9), one arrives at

$$\alpha_n = (2n + 1)\pi/(2L) \ (n = 0, 1, 2) \quad (10a)$$

and

$$A^c = \frac{C_2^c}{C_1^c}A_y + \left(e_{33} - \frac{c_{12}^c}{c_{11}^c}e_{31}\right)\frac{E_3}{C_1^c} \quad (10e)$$

where C_1^c, C_2^c, C_1^p, and C_2^p are defined in the Appendix. The superscripts p and c stand for polymer matrix and ceramic plate, respectively, and this convention will be used through out this paper. For the sake of simplicity, B_n^c and B_n^p are rewritten as

$$B_n^c = (A^c - A^p)B_{n0}^c$$
$$B_n^p = (A^c - A^p)B_{n0}^p$$

It is clear that B_{n0}^c and B_{n0}^p depend only on the properties of the composite and will not change with the experimental conditions.

Incidentally, $\beta_0^p = \frac{\pi}{2L}\sqrt{\frac{Y}{\mu}\frac{(2-\sigma)}{2(1-\sigma^2)}}$ in (9b), which is the prefactor in the cosh function of the first term describing the nonuniform strain profile in the polymer matrix in the x-direction, is quite similar to that obtained in our earlier analysis except there the strain in the z-direction is assumed

$$B_n^p = \frac{2(-1)^n}{L(\alpha_n)^2} \frac{(A^c - A^p)\left[\mu^c\left(K^c + \frac{c_{12}^c}{c_{11}^c K^c}\right)\sinh\left(\beta_n^c\frac{d}{2}\right)\right]}{\left(\mu^c\left(K^c + \frac{c_{12}^c}{c_{11}^c K^c}\right)\sinh\left(\beta_n^c\frac{d}{2}\right)\cosh\left(\beta_n^p\frac{a}{2}\right) + \mu^p\left(K^p + \frac{c_{12}^p}{c_{11}^p K^p}\right)\cosh\left(\beta_n^c\frac{d}{2}\right)\sinh\left(\beta_n^p\frac{a}{2}\right)\right)} \quad (10b)$$

$$B_n^c = \frac{2(-1)^{n+1}}{L(\alpha_n)^2} \frac{(A^c - A^p)\left[\mu^p\left(K^p + \frac{c_{12}^p}{c_{11}^p K^p}\right)\sinh\left(\beta_n^p\frac{a}{2}\right)\right]}{\left(\mu^c\left(K^c + \frac{c_{12}^c}{c_{11}^c K^c}\right)\sinh\left(\beta_n^c\frac{d}{2}\right)\cosh\left(\beta_n^p\frac{a}{2}\right) + \mu^p\left(K^p + \frac{c_{12}^p}{c_{11}^p K^p}\right)\cosh\left(\beta_n^c\frac{d}{2}\right)\sinh\left(\beta_n^p\frac{a}{2}\right)\right)} \quad (10c)$$

$$A^p = \frac{C_2^p}{C_1^p}A_y \quad (10d)$$

to be uniform [6], [7]. Since β_n^p describes the strain decay in the polymer phase in the x-direction, for more efficient stress transfer between the two constituents, a smaller β_n^p is preferred, which implies that the polymer should have a smaller Young's modulus and a large shear modulus. A composite with a larger L will also improve the stress transfer. These conclusions are the same as those derived from our earlier theoretical model [6], [7].

Finally, A_y can be determined from the force balance condition (Newton's third law) in the y-direction, which requires that the total force experienced by the ceramic plate should be equal in magnitude and opposite in sign to that in the polymer matrix

$$\int_0^L \int_{a/2}^{(a+d)/2} T_{yy}^c dx dz + \int_0^L \int_0^{a/2} T_{yy}^p dx dz = 0$$

From this

$$A_y = \frac{\mathrm{III}^E E_3}{\frac{L}{2}(dC_A^c + aC_A^p) - C_B(\mathrm{II}^c + \mathrm{II}^p)}$$

where C_A^c, C_A^p, C_B, II^c, II^c, and III^E are defined in the Appendix.

Equation (9) shows that the strain profile not only depends on the x-coordinate but also depends on the z-coordinate. The coupling between the polymer and ceramic changes the strain pattern in both directions.

In order to verify these theoretical results, the surface profiles of several 2-2 composites with different thickness $2L$ were measured using a double beam laser dilatometer. The 2-2 composites were made from PZT-500 ceramics [14] and Spurrs epoxy [15] with the dimensions of $a = 1.3$ mm and $d = 1.0$ mm. The 2-2 composite samples with different thicknesses $2L$ used in the surface profile measurement were cut from one original piece. Shown in Fig. 2 is the comparison of experimentally measured surface profiles with those calculated using (9) at the surface of the composites ($z = \pm L$). All the input parameters are fixed in the calculation, which are taken from the data either from the manufacturer or from the other measurements [14], [15]. During the process of making these 2-2 composite samples, there was some degree of depoling due to the heating of the ceramic plate to higher temperature. The d_{33} value was reduced from 400 pm/V (poled by the manufacturer) to a lower value of 356 pm/V and the d_{31} value was also reduced in the same proportion. In the theoretical calculation, these reduced values were used. For clarity, not all experimentally measured surface profiles are shown in Fig. 2. In Table I, the ratio of u_z^p at $x = 0$ to u_z^c at $x = (a+d)/2$ from all the samples measured and the corresponding theoretically calculated values are listed, since this is the most sensitive parameter reflecting the nonuniform strain distribution in the x-direction of a composite. Excellent agreement between the experimentally measured profiles and theoretically predicted ones was achieved over a large range of aspect ratio without adjustable parameters, and the theoretical fitting parameters (listed in Table II) agree with the earlier measured results. The results here also demonstrate that the surface profile becomes more or less uniform as the aspect ratio becomes large.

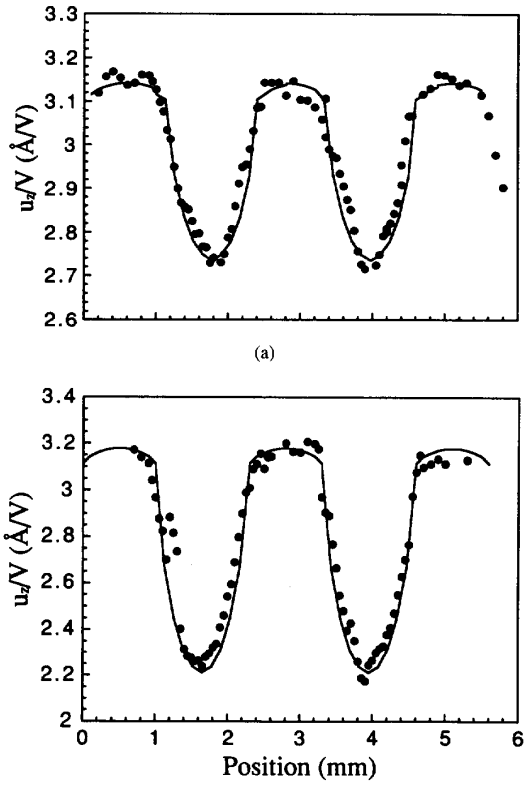

Fig. 2. Comparison between measured and calculated surface displacement profiles (in the x-direction) for a composite subjected to a low frequency electric field. The black dots are the experimental data points and the solid lines are theoretical results. The ceramic regions have a high displacement value than the polymer regions. The displacement profile of the composite was measured using a double beam laser dilatometer at a frequency of 250 Hz. The dimensions of the composites are $a = 1.3$ mm, $d = 1.0$mm, with (a) $2L = 10.4$ and (b) 4.3 mm, respectively.

TABLE I
THE COMPARISON OF EXPERIMENTALLY MEASURED AND THEROETICALLY CALCULATED NONUNIFORM STRAIN DISTRIBUTION OF 2-2 COMPOSITES ($d = 1.0$ mm, $a = 1.3$ mm)

L (mm)	u_z^p/u_z^c (exp.)	u_z^p/u_z^c (theo.)
5.2	0.88	0.87
4.06	0.84	0.836
3.1	0.79	0.787
2.15	0.72	0.70
1.35	0.5	0.538

Fig. 3 show the strain profile in the z-direction calculated using (9) for both ceramic plate and polymer matrix for three aspect ratios ($d/L = 0.4, 0.2$, and 0.05) with 40% ceramic content for 2-2 composites made of PZT-500 plates and Spurrs epoxy. The parameters used in the calculation are given in

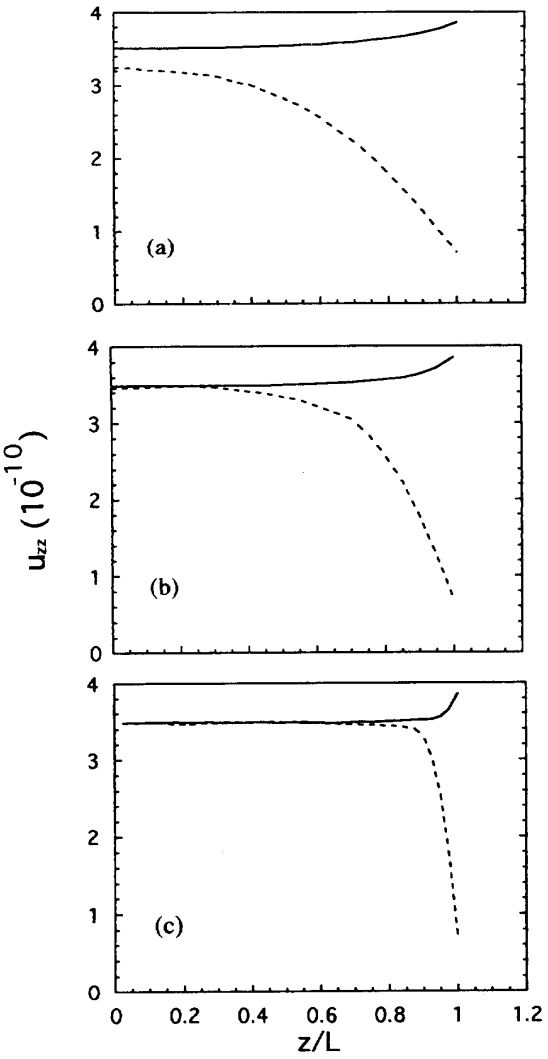

Fig. 3. The effect of the aspect ratio on the nonuniform strain profile in the z-direction for both ceramic plate $\overline{u^c_{zz}(z)}$ (solid lines) and polymer matrix $u^p_{zz}(z)$, (dashed lines). $\overline{u^c_{zz}(z)}$ is the average displacement of the ceramic plate and $u^p_{zz}(z)$ is the polymer displacement at $x = 0$, the applied electric field is 1 V/m along the z-direction, $a = 3$ mm and $d = 2$ mm with three different thicknesses: (a) $2L = 10$ mm; (b) $2L = 20$ mm; (c) $2L = 80$ mm.

Table II except $d_{33} = 400$ pm/V and $d_{31} = -175$ pm/V are used here. For the ceramic plate, the strain u_{zz} plotted is averaged over x, and for the polymer, the value was taken at $x = 0$:

$$\overline{u^c_{zz}} = A^c + \frac{2}{dK^c}\sum_{n=0}^{\infty} B^c_n \cos(\alpha_n z)\sinh[\beta^c_n d/2] \quad (11a)$$

$$u^p_{zz} = A^p + \sum_{n=0}^{\infty} B^p_n \alpha_n \cos(\alpha_n z) \quad (11b)$$

Figs. 2 and 3 show clearly that the strain depends both x and z. It also shows that near the surface the piezoelectric response of the ceramic plate is very close to that of pure ceramic ($d_{33} = 400$ pm/V) while the strain in the polymer near $z = L$ is nearly zero. In other words, the elastic coupling between the two phases does not affect very much the piezoelectric response of the ceramic plate and elastic response of the polymer matrix near the surface region ($z = \pm L$). On the other hand, although the strain in the z-direction shows large changes with z-coordinate for composites with a small aspect ratio, the strain in the z-direction is almost a constant for composites with large aspect ratio, for which the constant strain approximation in the z-direction and isostrain approximation in the x-direction should be appropriate. These results also justify the assumption made earlier in this paper that u_{yy} is a constant for a 2-2 composite since the y- dimension is much larger than the ceramic plate width d and polymer matrix gap a.

TABLE II
THE PARAMETERS USED FOR PZT-500 CERAMICS AND SPURRS EPOXY IN THE CALCULATION FOR TABLE I AND FIG. 2

PZT $Y^c = 5.43\ (10^{10}\ N/m^2)$, $\mu^c = 2.06\ (10^{10}\ N/m^2)$, $\sigma^c = 0.31$, $c_{11}{}^c = 1.156\ (10^{11}\ N/m^2)$
$c_{12}{}^c = 0.75\ (10^{11}\ N/m^2)$, $d_{33} = 356$ (pm/V), $d_{31} = -156$ (pm/V), $\varepsilon^c = 1700\ \varepsilon_0$

Spurrs Epoxy $Y^p = 4.8\ (10^9\ N/m^2)$, $\mu^p = 1.76\ (10^9\ N/m^2)$, $\sigma^p = 0.364$
$c_{11}{}^p = 8.27\ (10^9\ N/m^2)$, $c_{12}{}^p = 4.7\ (10^9\ N/m^2)$, $\varepsilon^p = 4\ \varepsilon_0$

III. PIEZOELECTRIC RESPONSE UNDER HYDROSTATIC PRESSURE

When a 2-2 piezoceramic polymer composite is subjected to a hydrostatic pressure ($-p$), the elastic response of both ceramic plate and polymer matrix is still described by (1), (2), and (3) except that (4) becomes

$$T_{xx} = c^c_{11}u_{xx} + c^c_{12}u_{yy} + c^c_{12}u_{zz} \quad (12a)$$

$$T_{yy} = c^c_{12}u_{xx} + c^c_{11}u_{yy} + c^c_{12}u_{zz} \quad (12b)$$

$$\text{and } T_{zz} = c^c_{12}u_{xx} + c^c_{12}u_{yy} + c^c_{11}u_{zz} \quad (12c)$$

for the ceramic plates. For the polymer matrix, one just replace c^c_{ij} in (11) by c^p_{ij}, the stiffness constant of the polymer phase used. From $T_{xx} = -p$, the relation between u_{xx} and u_{zz} becomes

$$u_{xx} = \frac{-1}{c_{11}}(p + c_{12}u_{zz} + c_{12}A_y)$$

which can be used for ceramic plates and polymer matrix.

The elastic displacement u_z for the two phases are those in (9a) and (9b). The boundary conditions now are

$$T_{zz} = -p \text{ at } z = \pm L,$$
$$u^c_{zz} = u^p_{zz} \text{ and } T^c_{xz} = T^p_{xz} \text{ at } x = a/2,$$
$$\text{and } u^c_{yy} = u^p_{yy} = A_y.$$

$\alpha_n = (2n+1)\pi/(2L)$, B^p_n, and B^c_n are those in (10a) and (10b). A^c, A^p, and A_y now are different from those in the electric field driven situation

$$A^c = \frac{-p}{c^c_{11} + c^c_{12}} + \frac{C^c_2}{C^c_1}A_y \quad (13a)$$

$$A^p = \frac{-p}{c^p_{11} + c^p_{12}} + \frac{C^p_2}{C^p_1}A_y \quad (13b)$$

Taking into account the external stress $(-p)$ in the y- direction, the force balance condition in that direction requires

$$\int_0^L \int_{a/2}^{(a+d)/2} T_{yy}^c dxdz + \int_0^L \int_0^{a/2} T_{yy}^p dxdz = -p(a + d)L/2 \tag{14}$$

where T_{yy}^p and T_{yy}^c are the stresses in the polymer matrix and ceramic plate, respectively. Equation (14) states that the total force experienced by the composite in the y-direction should be the same as that exerted by the hydrostatic pressure. Hence, the strain in the y-direction, A_y, can be determined from (14),

$$A_y = \frac{(\mathrm{III}^h - (a + d)L/2)p}{\frac{L}{2}(dC_A^c + aC_A^p) - C_B(\mathrm{II}^c + \mathrm{II}^p)} \tag{15}$$

where C_A^c, C_A^p, C_B, II^c, II^p, and III^h are all defined in the Appendix.

The nonuniform strains and stresses in the ceramic plate imply that the piezoelectric hydrostatic response in the ceramic is not uniform, it depends on both x and z coordinates. For example, the local piezoelectric hydrostatic response can be found from the relation

$$E_3 = -[g_{33}T_{zz} + g_{31}(T_{xx} + T_{yy})] = -g_h^{\mathrm{eff}}(-p) \tag{16}$$

where g_h^{eff} is introduced as the local effective piezoelectric hydrostatic coefficient, which is a function of both x and z coordinates. Utilizing the results derived above, one can get

$$E_3 = -\left[-p\left\{ g_{33}\frac{c_{12}^c}{c_{11}^c} + g_{31}\left(1 + \frac{c_{12}^c}{c_{11}^c}\right)\right\} + A_y(g_{31}c_1^c - g_{33}c_2^c) + u_{zz}^c(g_{33}C_1^c - g_{31}C_2^c)\right] \tag{17}$$

Apparently, the third term, which contains u_{zz}^c, is responsible for the variation of the hydrostatic response with x and z coordinates.

The z-dependence of the piezoelectric response predicted by (17) was verified experimentally. The local stress field was probed in a 2-2 composite with multilayer structure (see schematic in Fig. 4). The multilayer 2-2 composite was made of PZT-500 ceramic and Spurrs epoxy with total eleven layers. The ceramic plates were glued together using silver epoxy which also serves as electrodes for each layer. The charge output under an AC hydrostatic pressure (50 Hz) was measured for each layer with the electrodes of other layers shorted together. The experimentally measured quantity corresponds to $\overline{E_3}$, which is E_3 averaged over x on the ceramic plate

$$\overline{E_3} = -\left[-p\left\{ g_{33} + g_{31}\left(1 + \frac{2c_{12}^c}{c_{11}^c + c_{12}^c}\right)\right\} + A_y g_{31}\frac{(c_{11}^c + 2c_{12}^c)(c_{11}^c - c_{12}^c)}{c_{11}^c + c_{12}^c} + 2(g_{33}C_1^c - g_{31}C_2^c)\frac{(A^c - A^p)}{dK^c} \times \sum_{n=0}^{\infty} B_{n0}^c \cos(\alpha_n z)\sinh\left(\beta_n^c \frac{d}{2}\right)\right] \tag{18}$$

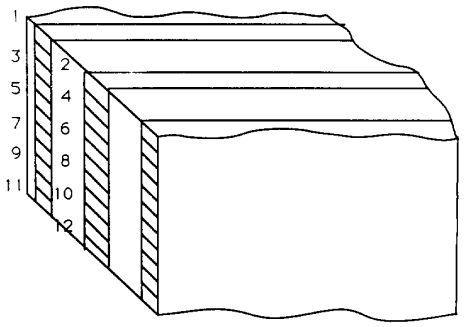

Fig. 4. Schematic drawing of the multilayer 2-2 composite, which consists of eleven ceramic layers glued together using silver epoxy with the thickness of each ceramic layer being 0.79 mm. The dimensions of the composite are: $a = 1.3$ mm, $d = 1.06$ mm, $2L = 8.7$ mm. The electrodes for each layer are numbered from 1 to12.

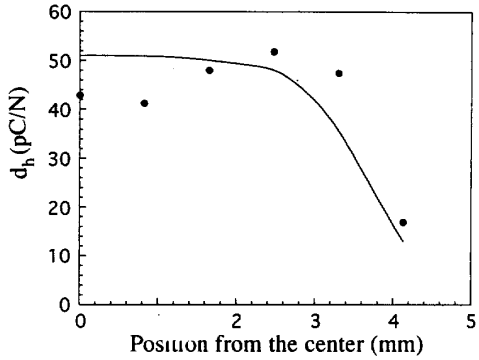

Fig. 5. The charge output from the electrode pairs: 1 and 2, 2 and 3, 3 and 4, 4 and 5, 5 and 6, 6 and 7 (shown in black dots) and their comparison with the theoretically calculated result (solid line). The data point at $z = 0$ is for pair 6 and 7 and the point near the composite surface ($z = 4.35$) is for pair 1 and 2. When the charge output, for example, from the second layer was measured (between the electrodes 2 and 3), the electrodes 1 and 2 were connected together and the electrodes 3 to 12 were also connected together.

The experimental result and theoretical calculation are compared in Fig. 5 and the agreement between the two is satisfactory.

The effective hydrostatic piezoelectric coefficient $\overline{g_h}$ of the sample can be found by averaging $\overline{E_3}$ in (18) over z $\left(E_3^{\mathrm{ave}} = \frac{1}{L}\int_0^L \overline{E_3}dz\right)$ and $\overline{g_h} = E_3^{\mathrm{ave}}/p$. $\overline{d_h}$ for the sample is $\overline{g_h}\bar{\varepsilon}$. $\bar{\varepsilon}$ is the averaged dielectric permitivity of a composite $\bar{\varepsilon} = v_c\varepsilon^c + (1 - v_c)\varepsilon^p$, where v_c is the volume content of ceramics in a composite, ε^c and ε^p are the dielectric permitivity of the ceramic plate and polymer, respectively. Usually, ε^c is much larger than ε^p, which results in $\bar{\varepsilon} = v_c\varepsilon^c$. Hence,

$$\overline{d_h} = v_c\gamma d_h \tag{19}$$

where

$$\gamma = \left[\left(d_{33} + d_{31}\left(1 + \frac{2c_{12}^c}{c_{11}^c + c_{12}^c}\right)\right) - \mathrm{III}^y\frac{(c_{11}^c - c_{12}^c)(c_{11}^c + c_{12}^c)}{c_{11}^c + 2c_{12}^c}d_{31}\right.$$

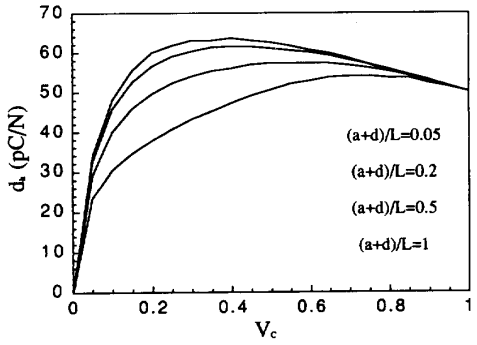

Fig. 6. The calculated piezoelectric hydrostatic constant $\overline{d_h}$ of 2-2 composites as a function of the ceramic volume content v_c for different aspect ratio. The parameters used in the calculation are listed in Table II except here $d_{33} = 400$ pm/V and $d_{31} = -175$ pm/V. The top curve is for $(a+d)/L = 0.05$ and the bottom one is for $(a+d)/L = 1$.

$$-\frac{2(d_{33}C_1^c - d_{31}C_2^c)}{dLC_2^c}(C_B\mathrm{III}^y + C_D)\mathrm{II}^c\Big]\Big/ d_h$$

where $d_h = (d_{33} + 2d_{31})$ is the hydrostatic piezoelectric coefficient of the ceramic plate, and γ is the stress transfer factor, which measures how much stress is transferred from the polymer matrix to ceramic plates. In Fig. 6, $\overline{d_h}$ is plotted against the ceramic content in the composite for different aspect ratio. The results for $(a+d)/L = 0.01$ and 0.05 are almost identical, which indicates that the aspect ratio effect saturates at $(a+d)/L \sim 0.05$. In other words, when L becomes larger, the results derived here approaches those derived from the isostrain approximation and there is no further improvement in the piezoelectric performance of a composite with a smaller $(a+d)/L$.

In Fig. 7, the tensile stress T_{zz} for a ceramic plate is plotted as a function of the z-coordinate for 2-2 composites with different aspect ratio. The ceramic content is kept at 40% and the composite is subjected to a hydrostatic pressure of 1 N/m^2. In the figure, T_{zz} is the average over $x = a/2$ to $x = a/2+d$. Most of the parameters used in the calculation are listed in Table II except $d_{33} = 400$ pm/V and $d_{31} = -175$ pm/V (the value for PZT-500 from the manufacturer) [14]. In Fig. 8, the strain u_{zz} as a function of z is plotted for both ceramic plate and polymer matrix [(11a) and (11b)]. The result is similar to that in Fig. 3 where the sample is under an electric field.

In order to have a stress transfer between the two phases in a composite, it is necessary that a strain gradient exists between the two phases in the x-direction. The larger this gradient is, the more the stress will be transferred between the two phases. Fig. 8 shows clearly that the stress transfer between the polymer matrix and ceramic plate mainly occurs near the surface of the composite ($z = \pm L$). For composites with large aspect ratio, the portion of polymer participating in the stress transfer is relatively small, i.e., most of the polymer does not contribute to the stress transfer. In fact, the polymer in the interior region acts only as the elastic loading which reduces the effective stress transfer between the two phases. Therefore, a composite with the polymer matrix made of very

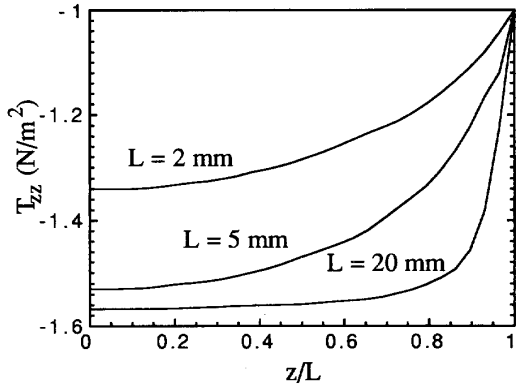

Fig. 7. The tensile stress T_c^{zz} for the ceramic plate as a function of z for 2-2 composites with different L. The ceramic width $d = 2$ mm and the width of polymer gap $a = 3$ mm. The composites are subjected to a hydrostatic pressure of $-1N/m^2$.

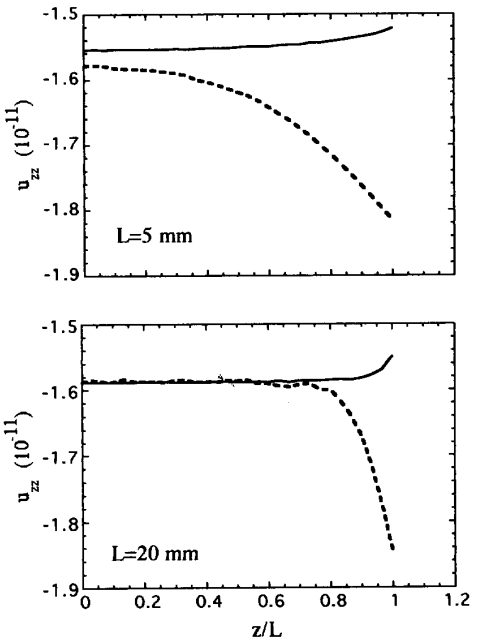

Fig. 8. The effect of the aspect ratio on the nonuniform strain profile in the z-direction for both ceramic plate $\overline{u_{zz}^c(z)}$ (solid line) and polymer matrix $u_{zz}^p(z)$ (dashed line), where $\overline{u_{zz}^c(z)}$ is that averaged over the ceramic plate and $u_{zz}^p(z)$ is at $x = 0$ when the composite is subjected to a hydrostatic pressure $-p = -1N/m^2$. The 2-2 composite has $a = 3$ and $d = 2$ mm, respectively.

stiff polymer near surface region (near $z = \pm L$), and very soft polymer in the interior (near $z = 0$) can have a much better piezoelectric performance.

IV. Summary

Starting from the basic elastic equations, the static piezoelectric performance of piezoceramic polymer composites with

2-2 connectivity has been analyzed theoretically. The results show that due to the elastic coupling between the two constituent phases, the strain is not only nonuniform in the x-direction, but also in the z-direction. Most of the stress transfer between the two phases occurs at the region near the surface of a composite, the materials in the interior of the composite does not contribute significantly to the stress transfer. The results confirm that the isostrain model may be used for composites with very large aspect ratio without introducing much error. In order to improve the piezoelectric performance of a composite, the composite should be made of polymer matrix with a small Young's modulus and a large shear modulus, and a large aspect ratio. It may be desirable to have the polymer matrix made of two different polymers with the stiffer one near the surface and the softer one in the interior of the composite.

Surface profiles of a series of 2-2 composite with different aspect ratio were measured using a double beam laser interferometer and the experimental results show excellent agreement with the theoretical calculations. The nonuniform strain in the z-direction of a composite was also confirmed by experiment.

It should be noted that these conclusions reached here are based on static elastic relations, they are valid only for low frequencies, that is, for frequencies well below various resonance modes in a composite. Similar analysis on the performance of a piezocomposite near its thickness resonance frequency will be pursued in the future.

APPENDIX

$$C_1^c = \left(c_{11}^c - \frac{(c_{12}^c)^2}{c_{11}^c}\right) \quad \text{and } C_2^c = -\left(c_{12}^c - \frac{(c_{12}^c)^2}{c_{11}^c}\right)$$

$$C_1^p = \left(c_{11}^p - \frac{(c_{12}^p)^2}{c_{11}^p}\right) \quad \text{and } C_2^p = -\left(c_{12}^p - \frac{(c_{12}^p)^2}{c_{11}^p}\right)$$

$$C_A^p = C_1^p - \frac{(C_2^p)^2}{C_1^p} \quad \text{and } C_A^c = C_1^c - \frac{(c_2^c)^2}{C_1^c}$$

$$C_B = \frac{C_2^c}{C_1^c} - \frac{C_2^p}{C_1^p}$$

$$C_D = \left(\frac{1}{c_{11}^p + c_{12}^p} - \frac{1}{c_{11}^c + c_{12}^c}\right)$$

$$\mathrm{II}^c = \sum_{n=0}^{\infty} C_2^c \frac{(-1)^n \sinh(\beta_n^c \frac{d}{2})}{\beta_n^c} B_{n0}^c$$

$$\mathrm{II}^p = \sum_{n=0}^{\infty} C_2^p \frac{(-1)^n \sinh(\beta_n^p \frac{d}{2})}{\beta_n^p} B_{n0}^p$$

$$\mathrm{III}^E = \frac{1}{C_c^1}\left(e_{33} - \frac{c_{12}^c}{c_{11}^c} e_{31}\right)(\mathrm{II}^c + \mathrm{II}^p) + \frac{Ld}{2}\left((1 - \frac{c_{12}^c}{c_{11}^c})e_{31} + \frac{C_2^c}{C_1^c}(e_{33} - \frac{c_{12}^c}{c_{11}^c} e_{31})\right)$$

$$\mathrm{III}^h = \left(\frac{1}{c_{11}^p + c_{12}^p} - \frac{1}{c_{11}^c + c_{12}^c}\right)(\mathrm{II}^c + \mathrm{II}^p) + aL(\frac{c_{12}^p}{c_{11}^p + c_{12}^p}) + dL(\frac{c_{12}^c}{c_{11}^c + c_{12}^c})$$

$$\mathrm{III}^y = \frac{\mathrm{III}^h - (a+d)L/2}{(dC_A^c + aC_C^p)L/2 - C_B(\mathrm{II}^c + \mathrm{II}^p)}$$

ACKNOWLEDGMENT

The authors wish to thank Dr. W. A. Smith, N. R. Sottos, and C. Richard for stimulating discussions.

REFERENCES

[1] R. E. Newnham, D. P. Skinner, and L. E. Cross, "Connectivity and piezoelectric-pyroelectric composites," *Mater. Res. Bull.*, vol. 13, pp. 525–536, 1978.
[2] W. A. Smith and B. A. Auld, "Modeling of 1–3 composites: Thickness-mode oscillations," *IEEE Trans. Ultrason., Ferroelec., Freq. Contr.*, vol. 38, pp. 40–47, 1991.
[3] K. A. Klicker, "Piezoelectric composites with 3–1 connectivity for transducer applications," Ph.D. Thesis, Penn State University, University Park, PA, 1980.
[4] T. R. Gururaja, A. Safari, R. E. Newnham, and L. E. Cross, "Piezoelectric ceramic-polymer composites for transduder applications," in *Electronic Ceramics*, L. M. Levinson, Ed. New York: Marcel Dekker, 1987, pp. 92–128.
[5] W. A. Smith, "Modeling of 1–3 composite piezoelectrics: Hydrostatic response," *IEEE Trans. Ultrason., Ferroelec., Freq. Contr.*, vol. 40, pp. 41–49, 1993.
[6] Q. M. Zhang, W. Cao, H. Wang, and L. E. Cross, "Strain profile and piezoelectric performance of piezocomposites with 2-2 and 1–3 connectivities," in *Proc. 1992 IEEE 8th Int. Symp. Appl. Ferroelec.* (ISAF8) at Clemson Univ., 1992, pp. 252–254.
[7] W. Cao, Q. M. Zhang, and L. E. Cross, "Theoretical study on the static perfromance of piezoelectric ceramic-polymer composites with 2-2 connectivity," *IEEE Trans. Ultrason.Ferroelec., Freq. Contr.*, vol. 40, pp. 103–109, 1993.
[8] L. D. Landau and E. M. Lifshotz, *Theory of Elasticity*. Oxford: Pergamon, 1986, 3rd ed.
[9] W. Nowacki, *Thermoelasticity*. Oxford: Pergamon, 1986, second ed.
[10] J. A. Nairn, "A variational mechanics analysis of the stress around breaks in embeded fibers," *Mach. of Mater.*, vol. 13, pp. 131–154, 1992.
[11] H. L. Cox, "The elasticity and strength of paper and other fibrous materials," *Br. J. Appl. Phys.*, vol. 3, pp. 72–79, 1952.
[12] A. Kelly and W. R. Tyson, "Fiber strengthened materials," *J. Mech. Phys. Solids*, vol. 10, pp. 329–350, 1963.
[13] Q. M. Zhang, S. J. Jang, and L. E. Cross, "High-frequency strain response in ferroelectrics and its measurement using a modified Mach-Zehnder interferometer," *J. Appl. Phys.*, vol. 65, pp. 2807–2813, 1989.
[14] PZT-500 is the trade-mark of Piezo Kinetics Inc. for one of its PZT ceramics. The data are from Data sheet of Piezo Kinetics Inc., Bellefonte, PA, 1992.
[15] C. G. Oakley, "Analysis and development of piezoelectric composites for medical ultrasound transducer applications," Ph.D. Thesis, Penn State University, University Park, PA, 1991.

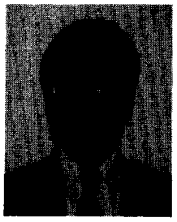

Q. M. Zhang was born in ZeiJian, China in 1957. He received the B.S. degree in physics from Nanjing University, China in 1981 and the Ph.D. degree, also in physics, from the Pennsylvania State University, University Park, in 1986.

He is currently an Assistant Professor of materials at Materials Research Laboratory of the Penn State University. His research interests involve piezoceramic and polymeric materials for sensor, actuator, and transducer applications; piezocomposites characterization and modeling; intelligent materials, structures, novel materials with large electromechanical effect, and nanocomposites; electrooptic properties and their applications; optical instrumentation; effects of defect structures on the dielectric, piezoelectric, and elastic properties of piezomaterials; and structural investigation of interface and defects in ferroelectrics. From 1986 to 1988, he was a research associate at Materials Research Laboratory as a research scientist, conducting research on interface, surface, and thin films as well as their phase transformation behavior with neutron and synchron X-ray scattering.

Dr. Zhang is a member of American Ceramic Society, American Physical Society, and Neutron Scattering Society of America.

Wenwu Cao was born on January 28, 1957 in Jilin, China. He received the B.S. degree in physics in 1982 from Jilin University, Changchun, China and the Ph.D. degree in condensed matter physics in 1987 from the Pennsylvania State University, University Park.

He was a Research Associate from 1987 to 1988, and then went to Cornell University, NY, as a post-Doctoral associate with the Laboratory of Atomic and Solid-State Physics in 1989. He rejoined the Pennsylvania State University as a member of the Research Faculty in 1990. He has conducted both theoretical and experimental research in the area of condensed matter physics, including theories on proper- and improper-ferroelastic phase transitions; static and dynamic properties of domain walls in ferroelectric and ferroelastic materialas. In addition, he has performed measurements on second- and third-order eleastic constants and piezolectric constants in ferroic single crystals and ceramics. His current interests are the formation of domain structures and their contributions to the dielectric, elastic, and piezolectric properties in ferroelectric ceramics, and the static and dynamic behavior of piezoelectric ceramic-polymer composites.

Dr. Cao is a member of the American Physical Society and the American Ceramic Society.

J. Zhao, photograph and biography not available at the time of publication.

L. E. Cross (SM'79–F'84), for a photograph and biography, see this issue, p. 421.